Available online at www.sciencedirect.com
SCIENCE DIRECT®
Bioorganic & Medicinal Chemistry Letters 14 (2004) 3425–3429
Bioorganic & Medicinal Chemistry Letters

Exploration of the P^2–P^3 SAR of aldehyde cathepsin K inhibitors

Eric E. Boros,[a] David N. Deaton,[a,*] Anne M. Hassell,[b] Robert B. McFadyen,[a] Aaron B. Miller,[b] Larry R. Miller,[c] Margot G. Paulick,[a,†] Lisa M. Shewchuk,[b] James B. Thompson,[a] Derril H. Willard, Jr.[d,✠] and Lois L. Wright[e]

[a]*Department of Medicinal Chemistry, GlaxoSmithKline, Five Moore Drive, Research Triangle Park, NC 27709-3398, USA*
[b]*Discovery Research Computational, Analytical, and Structural Sciences, GlaxoSmithKline, Five Moore Drive, Research Triangle Park, NC 27709-3398, USA*
[c]*Department of Molecular Pharmacology, GlaxoSmithKline, Five Moore Drive, Research Triangle Park, NC 27709-3398, USA*
[d]*Department of Gene Expression and Protein Biochemistry, GlaxoSmithKline, Five Moore Drive, Research Triangle Park, NC 27709-3398, USA*
[e]*Discovery Research Biology, GlaxoSmithKline, Five Moore Drive, Research Triangle Park, NC 27709-3398, USA*

Received 26 March 2004; accepted 24 April 2004

Abstract—The synthesis and biological activity of a series of aldehyde inhibitors of cathepsin K are reported. Exploration of the properties of the S^2 and S^3 subsites with a series of carbamate derivatized norleucine aldehydes substituted at the P^2 and P^3 positions afforded analogs with cathepsin K IC_{50}s between 600 nM and 130 pM.

Cathepsin K, a lysosomal cysteine protease of the C1A family highly expressed in osteoclasts, is crucial for the degradation of bone matrix.[1] Moreover, small molecule cathepsin K inhibitors are able to attenuate bone resorption in osteoporotic animal models.[2] As part of a broader goal of developing new therapeutics for osteoporosis, these researchers recently reported the discovery and P^1 SAR exploration of the aldehyde-based cathepsin K inhibitor **1** (Boc–Nle–H) derived from truncation of calpeptin (Cbz–Leu–Nle–H), which was identified in a focussed screen of known serine and cysteine protease aldehyde inhibitors.[3] This report will detail the further investigation of the SAR of this lead, concentrating on the P^2 and P^3 regions.

Two routes were utilized to synthesize P^2–P^3 aldehyde analogs. The first method converted commercially available P^2–P^3 alcohols **2a**–**c** and **2l** or known P^2–P^3 alcohol **2m**[4] into their chloroformates **3a**–**c** and **3l**–**m** mediated by phosgene as depicted in Scheme 1.[5] These

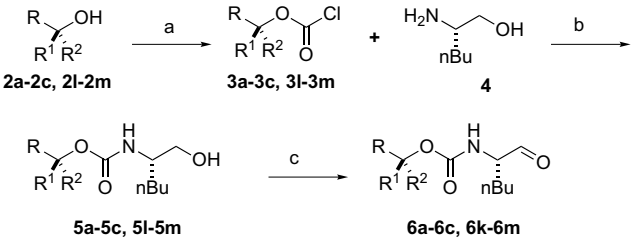

Scheme 1. (a) $COCl_2$, PhMe, 0 °C to rt; (b) iPr$_2$NEt, dioxane; (c) pyridine·SO_3, NEt_3, DMSO, CH_2Cl_2, −10 °C.

chloroformates were then coupled to the known amine **4**[6] to give the alcohols **5a**–**c** and **5l**–**m**.[7] Subsequent Moffatt oxidation of these alcohols **5a**–**c** and **5l**–**m** provided the desired aldehydes **6a**–**c** and **6k**–**m** after an extractive work-up.[8] The yields of the alcohols **5a**–**u** and aldehydes **6a**–**u** as well as the cathepsin K activity of the aldehyde analogs **6a**–**u** are shown in Table 1, while the yields of the alcohols **5v**–**z** and aldehydes **6v**–**z** as well as the cathepsin K activity of the aldehyde analogs **6v**–**z** are shown in Table 2.

Alternatively, the commercially available P^2–P^3 alcohols **2d**, **2f**, **2i**–**j**, and **2o**–**u**, the previously described P^2–P^3

* Corresponding author. Tel.: +1-919-483-6270; fax: +1-919-315-0430; e-mail: david.n.deaton@gsk.com
† Present address: Department of Chemistry, University of California—Berkeley, Berkeley, CA 94720-1460, USA.
✠ Deceased.

0960-894X/$ - see front matter © 2004 Elsevier Ltd. All rights reserved.
doi:10.1016/j.bmcl.2004.04.084

Table 1. P^2–P^3 cathepsin K inhibition and synthesis yields

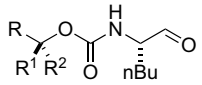

#	R	R^1	R^2	**5** yd. (%)	**6** yd. (%)	Cat. K IC_{50} (nM)[a]
1	Me	Me	Me	65	99	51
6a	Ph	H	H	65	99	540[b]
6b	$PhCH_2$	H	H	86	78	270[b]
6c	$Ph(CH_2)_2$	H	H	97	88	600[b]
6d	$PhCH_2$	Me	Me	93	67	12
6e	$PhCH_2$	$(CH_2)_3$		47	90	2.4
6f	$PhCH_2$	Et	Et	74	76	2.1
6g	$PhCH_2$	$(CH_2)_4$		63	80	0.35[c]
6h	$PhCH_2$	$(CH_2)_5$		45	95	2.0
6i	$PhCH_2$	Me	H	82	25	1.8
6j	$PhCH_2$	H	Me	86	88	100[d]
6k	$C_6H_{11}CH_2$	Me	H	77	94	2.7
6l	$PhCH_2$	Et	H	67	88	0.13[c]
6m	$PhCH_2$	*n*Pr	H	68	90	1.5
6n	$PhCH_2$	*i*Pr	H	88	80	0.50
6o	$PhCH_2$	*i*Bu	H	84	98	6.5
6p	$PhCH_2$	$PhCH_2$	H	88	99	71
6q	H	Et	Et	90	79	4.0
6r	H	*n*Pr	*n*Pr	90	85	0.87[c]
6s	H	*i*Pr	*i*Pr	81	96	0.56
6t	H	*i*Bu	*i*Bu	64	98	1.1
6u	Me	*i*Pr	*i*Pr	75	64	4.7[b]

[a] Inhibition of recombinant human cathepsin K activity in a fluorescence assay using 10 μM Cbz–Phe–Arg–AMC as substrate in 100 mM NaOAc, 10 mM DTT, 120 mM NaCl, pH = 5.5. The IC_{50} values are the mean of two or three inhibition assays, individual data points in each experiment were within a 2-fold range of each other.
[b] These entries represent an *n* of one.
[c] Individual data points in each experiment were within a 3-fold range of each other.
[d] This analog was synthesized from a commercially available chiral alcohol **2j**. It cannot be ruled out that the activity of **6j** might arise from contamination by a small amount of **6i** derived from starting alcohol **2j** being less than 100% enantiomerically pure.

Table 2. P^3 cathepsin K inhibition and synthesis yields

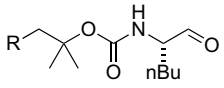

#	R	**5** yd. (%)	**6** yd. (%)	Cat. K IC_{50} (nM)[a]
6v	3-MeO–Ph	99	98	5.4[b]
6w	4-MeO–Ph	69	78	2.9
6x	2-Cl–Ph	77	77	3.1
6y	4-Cl–Ph	81	93	4.6[b]
6z	3-Thiophenyl	85	99	7.6[b]

[a] Inhibition of recombinant human cathepsin K activity in a fluorescence assay using 10 μM Cbz–Phe–Arg–AMC as substrate in 100 mM NaOAc, 10 mM DTT, 120 mM NaCl, pH = 5.5. The IC_{50} values are the mean of two or three inhibition assays, individual data points in each experiment were within a 2-fold range of each other.
[b] These entries represent an *n* of one.

alcohols **2e**,[9] **2g–h**,[10] **2n**,[11] and **2w–y**,[12–14] or the novel alcohols **2v**[15] and **2z**[16] were coupled to the known isocyanate **7**[17] to give the carbamates **8d–j** and **8n–z** as shown in Scheme 2.[18] Then, hydrolysis of the resulting esters **8d–j** and **8n–z**, followed by sodium borohydride-mediated reduction of the in situ generated mixed anhydrides provided the alcohols **5d–j** and **5n–z**.[19] The cyclohexyl alcohol **5k** was synthesized by hydrogenation

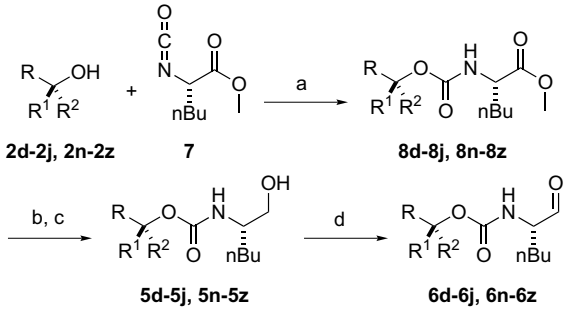

Scheme 2. (a) PhMe, 90 °C, 22–99%; (b) LiOH, THF, H_2O; (c) *i*PrOCOCl, NEt_3, THF, −10 °C; $NaBH_4$, H_2O, 0 °C; (d) pyridine·SO_3, NEt_3, DMSO, CH_2Cl_2, −10 °C.

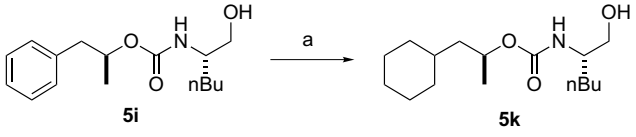

Scheme 3. (a) H_2, $RhCl_3·H_2O$, Aliquat® 336, $ClCH_2CH_2Cl$, H_2O (77%).

of the aryl ring of alcohol **5i** catalyzed by rhodium under phase transfer conditions as displayed in Scheme 3.[20]

Once again, the alcohols **5d–j** and **5n–z** were oxidized to the desired aldehydes **6d–j** and **6n–z**.

The lead aldehyde **1** contains no P^3 residue. With an X-ray crystal structure of cathepsin K unavailable at the start of this work, a traditional structure activity relationship study was employed. It was thought that the incorporation of an appropriately placed aryl substituent could result in favorable π–π stacking interactions with potential aryl groups in the S^3 subsite or the active site trough that accommodates the substrate backbone. To test this hypothesis, a potential S^3-binding phenyl ring was attached to the amino acid backbone with tethers of varying lengths.[21] The benzyl, phenethyl, and phenpropyl derivatives **6a–c** (cathepsin K IC_{50}s of 540, 270, and 600 nM, respectively, as shown in Table 1) did not differ significantly from each other in their ability to inhibit cathepsin K, nor did they offer increased potency over the aldehyde lead **1**.

Since the primary determinant of specificity of papain family endopeptidases is the S^2 pocket,[22] the *gem*-dimethyl P^2 group of lead **1** was combined with the phenyl P^3 moiety of **6b** to provide inhibitor **6d** ($IC_{50} = 12$ nM). This analog was ~4-fold more potent than analog **1** and ~20-fold more potent than analog **6b**. The *gem*-diethyl P^2 analog **6f** was then prepared and found to be even more active ($IC_{50} = 2.1$ nM). To further investigate the dimensions of the S^2 pocket, the cyclobutyl, cyclopentyl, and cyclohexyl P^2 moieties were incorporated with the P^3 phenyl group to afford inhibitors **6e** and **6g–h**. The cyclobutyl and cyclohexyl-containing compounds **6e** ($IC_{50} = 2.4$ nM) and **6h** ($IC_{50} = 2.0$ nM) were similar in inhibitory potency to the *gem*-diethyl analog **6f**, whereas the cyclopentyl-containing compound **6g** provided a 6-fold increase in potency ($IC_{50} = 0.35$ nM).

Although the incorporation of geminal disubstitution in the P^2 region afforded potent cathepsin K inhibitors, it was not clear if both P^2 substituents were required for favorable interactions with the enzyme. To address the contribution of each substituent to protease inhibition, the diastereomers **6i** and **6j** were synthesized. The (*S*)-methyl derivative **6i** ($IC_{50} = 1.8$ nM) exhibited substantially more inhibitory activity versus cathepsin K than its (*R*)-epimer ($IC_{50} = 100$ nM). Furthermore, analog **6i** was more potent than the *gem*-dimethyl derivative **6d**, demonstrating that the interaction of the inhibitor with cathepsin K in the S^2 pocket is stereospecific. Furthermore, a second geminal substituent is not only unnecessary, but can be detrimental to the inhibitory activity.

The interactions of the inhibitors with the S^3 domain of cathepsin K were further explored. Replacement of the P^3 phenyl group by a cyclohexyl moiety as in **6k** ($IC_{50} = 2.7$ nM) did not affect the inhibitory activity. Furthermore, as shown in Table 2, a five-membered heteroaryl ring as in **6z** could replace the phenyl ring with no loss in activity. Substitutions at the 2-, 3-, or 4-position of the phenyl group in the P^2 *gem*-dimethyl series by electron donating (**6v–w**) or electron withdrawing groups (**6x–y**) were all well tolerated. The absence of strong effects on the inhibitory activity by these P^3 changes suggests that the interactions of these substituents with the protein are quite weak.

Since the introduction of larger P^2 moieties resulted in increased inhibitory potency in the *gem*-disubstituted analogs and only the pro-(S) substituent was important for activity, further exploration of bigger P^2 alkyl groups in the more active diastereomer series was warranted. To that end, analogs of **6i** bearing larger P^2 alkyl groups were synthesized. The ethyl- and *iso*-propyl-containing analogs **6l** ($IC_{50} = 0.13$ nM) and **6n** ($IC_{50} = 0.50$ nM) were more potent inhibitors of cathepsin K than the methyl analog **6i**, whereas the *n*-propyl- and *iso*-butyl-containing derivatives **6m** ($IC_{50} = 1.5$ nM) and **6o** ($IC_{50} = 6.5$ nM) were approximately equipotent to the methyl analog **6i**. However, introduction of the larger benzyl group in compound **6p** ($IC_{50} = 71$ nM) resulted in a significant decrease in inhibitory activity. It is probably too large to be reasonably accommodated in the S^2 pocket.

In an attempt to avoid the added synthetic complexity associated with the incorporation of a second stereocenter, a group of symmetrical alcohols was used to prepare a series of inhibitors containing achiral P^2–P^3 moieties (compounds **6q–u**). The diethyl-, di-*n*-propyl-, di-*iso*-propyl-, and di-*iso*-butyl-containing analogs **6q–t** were more potent than the dibenzyl analog **6p** discussed above, and exhibited activity similar to the P^2-methyl P^3-benzyl analog **6i**. Addition of a methyl group to afford the methyl, di-*iso*-propyl-containing derivative **6u** ($IC_{50} = 4.7$ nM) did not enhance activity over **6s** ($IC_{50} = 0.56$ nM). Presumably, in these symmetrical inhibitors, one of the side chains occupies the S^2 pocket, whereas the second side chain lies in the active site trough that accommodates the substrate backbone.

Selectivity is a critical concern when designing potential therapeutics to avoid undesired side effects. Given the high degree of homology between the lysosomal cysteine cathepsins, achieving reasonable selectivity can be a daunting task. To ascertain the selectivity of this class of aldehyde inhibitors, selected analogs were screened against the commercially available cathepsins B and L with data shown in Table 3. Gratifyingly, all of these aldehyde inhibitors exhibit more inhibitory activity versus cathepsin K than against cathepsins B and L. Although several of the inhibitors were greater than 100-fold selective for cathepsin K versus the other two enzymes, in general, the cycloalkyl-containing inhibitors **6e**, **6g**, and **6h** were the more selective. The cyclohexyl-containing derivative **6h** is >6000-fold selective for cathepsin B and >4000-fold selective for cathepsin L. Interestingly, the diethyl-bearing analog **6f** (cathepsin L $IC_{50} = 110$ nM) is a substantially more potent inhibitor of cathepsin L than are the cycloalkyl-containing analogs **6e**, **6g**, and **6h**, whereas the mono-ethyl compound **6l** (cathepsin L $IC_{50} = 15$ nM) is even more potent. Analog **6l** is also a reasonably good inhibitor of cathepsin B (cathepsin B $IC_{50} = 72$ nM).

Table 3. Cathepsin B, K, and L inhibition and selectivity

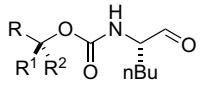

#	R	R^1	R^2	Cat. B IC_{50} (nM)[a]	Cat. K IC_{50} (nM)[a]	Cat. L IC_{50} (nM)[a]
6e	$PhCH_2$	$(CH_2)_3$		3400	2.4	1200
6f	$PhCH_2$	Et	Et	2200	2.1	110[c]
6g	$PhCH_2$	$(CH_2)_4$		810	0.35[c]	2000
6h	$PhCH_2$	$(CH_2)_5$		12,000	2.0	8500
6i	$PhCH_2$	Me	H	460	1.8	740
6k	$C_6H_{11}CH_2$	Me	H	400[b]	2.7	270[b]
6l	$PhCH_2$	Et	H	72[c]	0.13[c]	15[c]

[a] Inhibition of recombinant human cathepsin B, K, and L activity in a fluorescence assay using Cbz–Phe–Arg–AMC as substrate (cathepsins B and K (10 μM), cathepsin L (5 μM)) in 100 mM NaOAc, 10 mM DTT, 120 mM NaCl, pH = 5.5. The IC_{50} values are the mean of two or three inhibition assays, individual data points in each experiment were within a 2-fold range of each other.
[b] These entries represent an *n* of one.
[c] Individual data points in each experiment were within a 3-fold range of each other.

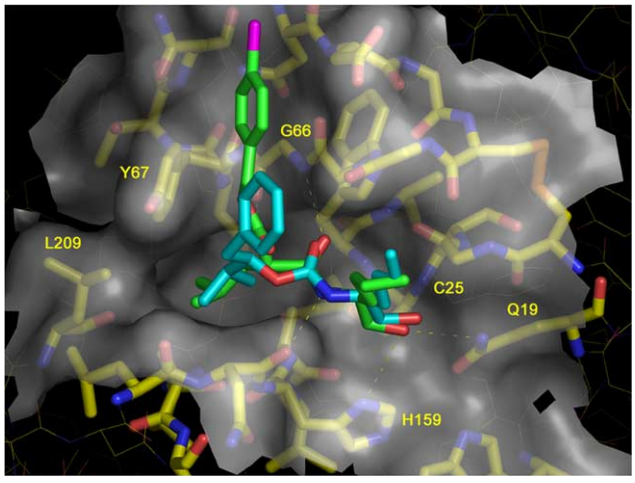

Figure 1. Active site of the X-ray co-crystal structure of compound **9** bound to cathepsin K. The cathepsin K carbons are colored yellow with inhibitor **9** carbons colored green. The semi-transparent white surface represents the molecular surface, while hydrogen bonds are depicted as yellow dashed lines. Inhibitor **6n**, with its carbons colored cyan, was modeled into the X-ray co-crystal structure, illustrating the probable mode of binding of these truncated aldehydes inhibitors. The coordinates have been deposited in the Brookhaven Protein Data Bank, accession number 1SNK. This figure was generated using PYMOL version 0.93.

The original lead for this aldehyde series identified by focussed screening was calpeptin, Cbz–Leu–Nle–H.[3] As part of an effort to obtain X-ray co-crystal structures of cathepsin K/inhibitor complexes, several heavy atom calpeptin derivatives were synthesized to assist in phasing the X-ray diffraction data. Co-crystallization of one of these analogs, *para*-bromo–Cbz–Leu–Nle–H **9** ($IC_{50} = 0.25$ nM),[23] with cathepsin K gave diffraction quality crystals, allowing the determination of the crystal structure. The X-ray co-crystal structure of bromine derivative **9** bound to cathepsin K, of which the active site is shown in Figure 1, gives some insights into the SAR of these P^2–P^3 analogs described above. The *iso*-butyl group is bound in a deep S^2 pocket formed by residues ^{67}Tyr, ^{68}Met, ^{134}Ala, ^{163}Ala, and ^{209}Leu. Hydrophobic groups should be preferred based on the lipophilic nature of these residues, and this was confirmed by these SAR studies.

Other interactions also contribute to the binding of these inhibitors. The S^1 binding site is created by residues ^{23}Gly, ^{24}Ser, ^{64}Gly, and ^{65}Gly and may be described as a wall rather than pocket since one half of the subsite is solvent exposed. All of the polar backbone atoms that form the wall are hydrogen bonded, which results in the subsite having a very hydrophobic character, explaining the preference for linear hydrophobic substituents in this position. The S^3 pocket consists of a 'groove' that is formed by ^{60}Asn, ^{61}Asp, ^{66}Gly, and ^{67}Tyr. It too has hydrophobic character and accommodates lipophilic substituents. A covalent hemithioketal intermediate is formed by the aldehyde of the inhibitor and the active site cysteine (^{25}Cys) of the protein. The OH of the hemithioketal is stabilized by three hydrogen bonds: (1) to the backbone amide of ^{25}Cys; (2) to the side chain of ^{19}Gln; and (3) to the side chain of catalytic ^{159}His. Two other hydrogen bonds formed between the inhibitor and the protease occur in the peptide recognition site; the NH and carbonyl oxygen of the inhibitor carbamate form hydrogen bonds to the backbone carbonyl of ^{161}Asn and the backbone HN of ^{66}Gly, respectively.

Analog **6n** ($IC_{50} = 0.50$ nM) is also depicted in Figure 1. This analog has been modeled into the active site of the enzyme utilizing the program MVP.[24] The inhibitor **6n** was docked into the active site by growing the ligand in the covalently attached state, starting at the β-carbon of ^{25}Cys. It illustrates the probable binding mode of this single amino acid aldehyde inhibitor class. As shown, there is good overlap between the modeled *iso*-propyl P^2 moiety of **6n** and the bound *iso*-butyl P^2 fragment of **9** in the S^2 pocket. The docked aldehyde inhibitor backbone of **6n** also maps well to the bound backbone of **9**. The P^1 substituents of these two inhibitors also show good agreement in the S^1 groove of the enzyme. The docked inhibitor **6n** has the P^3 moiety exposed to solvent with little if any interaction with the protease. Whereas this model is in good agreement with the P^3 SAR of these inhibitors, in that changes in P^3 had minimal effects on

the cathepsin K inhibitor potency, a comparison of analogs **6l** ($IC_{50} = 0.13$ nM) and **6q** ($IC_{50} = 4.0$ nM) shows that the P^3 moiety does contribute to inhibitor binding interactions. Although the data do not support the original hypothesis that P^3 aryl groups could form π–π stacking interactions in S^3, P^3–S^3 hydrophobic interactions do account for additional inhibitory activity, suggesting that the P^3 group of the docked inhibitor **6n** needs further refinement.

Aldehydes have a reputation for metabolic and chemical instability.[25] Not surprisingly, then, in vitro incubations with rat S9 liver homogenates revealed that these aldehyde inhibitors were rapidly degraded.[26] These results were supported by in vivo experiments in male Han Wistar rats. After dosing (iv dose = 5 mg/kg or po dose = 10 mg/kg), the plasma concentration of a P^1 derivative of aldehyde **6k** fell below the assay detection limit (<3 ng/mL) after 15 min, indicating rapid elimination in vivo. The poor pharmacokinetic properties of this class of aldehyde inhibitors precluded further in vivo pharmacodynamic studies. In spite of these disappointing, but not unexpected results, the SAR gleaned from this investigation and structural insight gained from the cathepsin K/inhibitor co-crystal structure proved valuable for the design of better inhibitors.

In summary, a series of aldehyde inhibitors of cathepsin K with varied substituents at the P^2 and P^3 positions were synthesized. Starting from aldehyde lead **1**, a P^3 moiety was introduced into the inhibitor and the P^2 substituent was optimized to produce picomolar cathepsin K inhibitors such as **6g**, **6l**, and **6s**. Analog **6g** was also very selective for inhibiting cathepsin K versus cathepsins B and L. Information gained from these SAR studies proved useful in the design of other cathepsin K inhibitors containing more metabolically stable thiol-reactive groups. The properties of these inhibitors will be reported in due course.

References and notes

1. Yamashita, D. S.; Dodds, R. A. *Curr. Pharm. Des.* **2000**, *6*, 1.
2. Stroup, G. B.; Lark, M. W.; Veber, D. F.; Bhattacharyya, A.; Blake, S.; Dare, L. C.; Erhard, K. F.; Hoffman, S. J.; James, I. E.; Marquis, R. W.; Ru, Y.; Vasko-Moser, J. A.; Smith, B. R.; Tomaszek, T.; Gowen, M. *J. Bone Miner. Res.* **2001**, *16*, 1739.
3. Catalano, J. G.; Deaton, D. N.; Furfine, E. S.; Hassell, A. M.; McFadyen, R. B.; Miller, A. B.; Miller, L. R.; Shewchuk, L. M.; Willard, D. H.; Wright, L. L. *Bioorg. Med. Chem. Lett.* **2004**, *14*, 275.
4. Berk, S. C.; Yeh, M. C. P.; Jeong, N.; Knochel, P. *Organometallics* **1990**, *9*, 3053.
5. Vedejs, E.; Wang, J. *Org. Lett.* **2000**, *2*, 1031.
6. Lingibe, O.; Graffe, B.; Sacquet, M.-C.; Lhommet, G. *Heterocycles* **1994**, *37*, 1469.
7. Wuts, P. G. M.; Pruitt, L. E. *Synthesis* **1989**, 622.
8. Luly, J. R.; Hsiao, C. N.; BaMaung, N.; Plattner, J. J. *J. Org. Chem.* **1988**, *53*, 6109.
9. Bernardon, C.; Deberly, A. *J. Org. Chem.* **1982**, *47*, 463.
10. Newkome, G. R.; Allen, J. W.; Anderson, G. M. *J. Chem. Educ.* **1973**, *50*, 372.
11. Souppe, J.; Danon, L.; Namy, J. L.; Kagan, H. B. *J. Organomet. Chem.* **1983**, *250*, 227.
12. Collins, S.; Hong, Y.; Hoover, G. J.; Veit, J. R. *J. Org. Chem.* **1990**, *55*, 3565.
13. Ferrari, G. *Farmaco, Edizione Scientifica* **1960**, *15*, 337.
14. Langhals, H.; Range, G.; Wistuba, E.; Ruechardt, C. *Chem. Ber.* **1981**, *114*, 3813.
15. The alcohol **2v** was synthesized from 3-methoxyphenylacetone and methyl magnesium bromide in 82% yield.
16. The alcohol **2z** was synthesized from ethyl thiophene-3-acetate and methyl magnesium bromide in 72% yield.
17. Effenberger, F.; Drauz, K. *Angew. Chem.* **1979**, *91*, 504.
18. Jeschkeit, H.; Losse, G.; Neubert, K. *Chem. Ber.* **1966**, *99*, 2803.
19. Kubota, M.; Nagase, O.; Yajima, H. *Chem. Pharm. Bull.* **1981**, *29*, 1169.
20. Blum, J.; Amer, I.; Zoran, A.; Sasson, Y. *Tetrahedron Lett.* **1983**, *24*, 4139.
21. Waters, M. L. *Curr. Opin. Chem. Biol.* **2002**, *6*, 736.
22. Turk, D.; Guncar, G.; Podobnik, M.; Turk, B. *Biol. Chem.* **1998**, *379*, 137.
23. Calpeptin derivative **9** was synthesized by a carbodiimide coupling of the known 4-bromo-benzyloxycarbonylleucine with amino alcohol **4**, followed by a Moffatt oxidation of the alcohol to provide the desired aldehyde in 78% yield.
24. Lambert, M. H. In *Practical Application of Computer-Aided Drug Design*; Charifson, P. S., Ed.; Marcel Dekker: New York, NY, 1997; p 243.
25. Blume, H.; Oelschlaeger, H. *Arzneim.-Forsch.* **1978**, *28*, 956.
26. Iwatsubo, T.; Hirota, N.; Ooie, T.; Suzuki, H.; Shimada, N.; Chiba, K.; Ishizaki, T.; Green, C. E.; Tyson, C. A.; Sugiyama, Y. *Pharmacol. Ther.* **1997**, *73*, 147.